ELSEVIER

Physica A 257 (1998) 61–76

PHYSICA A

Conformational structure of amphiphilic copolymers in dilute solution

Yu.A. Kuznetsov, E.G. Timoshenko *, K.A. Dawson [1]

Theory and Computation Group, Irish Centre for Colloid Science and Biomaterials[2], *Department of Chemistry, University College Dublin, Belfield, Dublin 4, Ireland*

Abstract

We present the equations of the extended Gaussian self-consistent method for study of equilibrium and kinetics of conformational transitions of arbitrary copolymer solutions. As applications of the method we consider the effect of the chain topology on the kinetics of homopolymer folding, sequence dependence of the phase diagram and folding kinetics of a single copolymer chain, and stability of mesoglobules in dilute polymer solutions.

PACS: 61.25.Hq; 64.60.My; 64.70.Pf; 01.30.Cc
Keywords: Macromolecular and polymer solutions; Metastable phases; Glass transitions

1. Introduction

Understanding copolymer solutions at various concentrations [1–3] is important for many applications in biochemistry, pharmaceutical and food sciences. The variety of conformational transitions and structures that could be formed in them is really amazing for copolymers with sufficiently complex sequences.

In the limit of infinite dilution one is interested in explaining the mysteries of folding of proteins, nucleic acids and other biopolymers. Conformational changes at nonequilibrium conditions present especial interest here as many of the structures resulting from polymer interactions in a cell appear and can exist only as a result of special kinetic processes. These problems have stimulated a renewed attention to studying the

* Corresponding author. Internet: http://fiachra.ucd.ie/~timosh.
[1] Author who presented the talk at the conference.
[2] Established at University College Dublin and Queen's University of Belfast.

0378-4371/98/$19.00
PII: S0378-4371(98)00128-9

fundamental kinetic laws of homopolymer collapse transition for a single chain and their extension to block and random copolymers. Although computer simulations are very valuable tools in this area, important progress in understanding such systems in kinetics has been achieved in the framework of the Gaussian self-consistent (GSC) method [4,5]. The latter presents a natural extension to kinetics of the variational Gibbs–Bogoliubov variational method.

At the high concentration end one would like to understand such conformational transitions as, for example, kinetics of phase separation leading to formation of complex morphologies and gelation due to hydrophobic association. The main theoretical progress in attacking these difficult problems has been so far made using mean-field-type approaches [6]. These, however, are not suitable for addressing nonequilibrium situations. Moreover, one may seriously doubt whether they are adequate for description of complex inhomogeneous systems. Relatively little is also known about the structures that could be formed within the two-phase separation region for copolymer solutions at sufficiently low concentrations. The experimental study in this region is impeded by difficulties in controlling aggregation in light scattering experiments [7].

We have recently shown that the GSC method can be successfully applied to multiple homopolymers in solution as well [8], and that the GSC equations in some approximation can be reduced to those of the Flory–Huggins theory. In addition, we have found a metastable state of mesoglobules that are formed by association of a few distinct chains. Such nano-sized mesoglobules are characterised by a rather monodisperse size distribution and are seen to remain stable for many hours in experiments with PNIPAM solutions [9,10]. In Ref. [11] we have mentioned a possibility that for copolymers these mesoglobules are additionally stabilised by the micro-phase separation, what has been confirmed experimentally in a recent work [12].

In this paper we present the GSC method in its most general form [13,11] that allows us to consider many interesting applications that could not be studied within the previous simplified treatments based on the kinematic symmetry assumptions for block copolymers [5].

2. The model and the method

We denote by $\mathbf{X}_n^a$ the spatial coordinates of the nth monomer in the ath chain and by $\mathbf{R}_i$ the spatial coordinates of the ith solvent molecule. The multi-index A denotes both the inter- and intra-chain indices n and a. The effective free energy functional of the system is

$$H_{ms} = H_{sol}[\mathbf{R}_\alpha] + H_{mon}[\mathbf{X}_n^a] - \sum_{A,i} I_A \, \delta(\mathbf{X}_A - \mathbf{R}_i) \, . \tag{1}$$

The last term in Eq. (1) describes contact interactions between monomers and the solvent, I_A being the monomer–solvent coupling constants. The monomer–monomer

contribution to the effective free energy functional (1) is given by

$$H_{mon} = \frac{k_B T}{2L^2} \sum_a (\mathbf{Y}^a - \mathbf{Y})^2 + \frac{k_B T}{2l^2} \sum_{a,n} (\mathbf{X}_n^a - \mathbf{X}_{n-1}^a)^2 + \frac{k_B T\, \lambda}{2l^3} \sum_{a,n} (\mathbf{X}_{n+1}^a + \mathbf{X}_{n-1}^a - 2\mathbf{X}_n^a)^2 + \sum_{J \geqslant 2} \sum_{\{A\}} u_{\{A\}}^{(J)} \prod_{i=1}^{J-1} \delta(\mathbf{X}_{A_{i+1}} - \mathbf{X}_{A_1}) , \tag{2}$$

where the centre of mass of a chain and all system is $\mathbf{Y}^a \equiv (1/N) \sum_n \mathbf{X}_n^a$, and $\mathbf{Y} \equiv (1/M) \sum_a \mathbf{Y}^a$. The first term above introduces a soft spatial cut-off L onto the system, the second and third terms correspond to the connectivity and bending contributions, l and λ being the statistical segment length and the persistent length of the chain, respectively. The volume interactions are represented by a virial-type expansion in the last term in Eq. (2). The virial coefficients $u_{\{A\}}^{(J)}$ are allowed to be arbitrary to describe the most general case of any mixture of heteropolymers with any composition.

Using the solution incompressibility condition, $\rho_{mon}(\mathbf{y}) + \rho_{sol}(\mathbf{y}) = \rho_0 = const$, one can integrate out the solvent degrees of freedom. The effect of the solvent influence on the polymer appears via the term, $H_{ms} = (\frac{1}{2}) \sum_{AA'} (I_A + I_{A'}) \delta(\mathbf{X}_A - \mathbf{X}_{A'})$. Thus, the solvent can be excluded from the consideration by shifting the second virial coefficient, $u_{AA'}^{(2)} \to u_{AA'}^{(2)} + (I_A + I_{A'})/2$. Here we consider amphiphilic heteropolymers, for which monomers differ only in their interactions with the solvent, $u_{AA'}^{(2)} = \bar{u}^{(2)} + (\Delta/2)(\sigma_A + \sigma_{A'})$, and $u_{\{A\}}^{(J)} = u^{(J)}$ for $J > 2$. The mean second virial coefficient, $\bar{u}^{(2)}$, is associated with the quality of the solvent and the parameter Δ is called the degree of amphiphilicity of the chain. The set $\{\sigma_n\}^a$ expresses the chemical composition, or the primary sequence, of a heteropolymer.

The long time scale evolution of the system is well represented by the Langevin equation

$$\frac{d}{dt} X_A^\alpha(t) = \sum_{\alpha', A'} \mathscr{H}_{AA'}^{\alpha\alpha'} [X(t)] \left(-\frac{\partial H}{\partial X_{A'}^{\alpha'}} + \eta_{A'}^{\alpha'}(t) \right) , \tag{3}$$

where $\mathscr{H}_{A\,A'}^{\alpha\,\alpha'}$ is the Oseen hydrodynamic interaction tensor and $\eta_A^\alpha(t)$ is the Gaussian noise with the second momentum, $\langle \eta_A^\alpha(t) \eta_{A'}^{\alpha'}(t') \rangle = (\mathscr{H}^{-1})_{A\,A'}^{\alpha\,\alpha'}\, 2k_B T\, \delta(t - t')$.

The main idea of the GSC method is to replace the nonlinear Langevin equation (3) by a linear stochastic equation with coefficients chosen according to the criterion

$$\frac{d}{dt} \mathbf{X}_A = -\sum_{A'} V_{AA'}(t)\, \mathbf{X}_{A'} + \eta_A(t), \qquad \left\langle \mathbf{X}_A \frac{\partial H}{\partial \mathbf{X}_{A'}} \right\rangle_0 = \left\langle \mathbf{X}_A \frac{\partial H_0}{\partial \mathbf{X}_{A'}} \right\rangle_0 , \tag{4}$$

with the trial Hamiltonian as the most general quadratic form, $2H_0 = \sum_{AA'} V_{AA'}(t)\mathbf{X}_A\mathbf{X}_{A'}$, with coefficients $V_{AA'}(t)$ depending on the chain indices A, A' and time t. One can show that the inter-molecular coordinates $\mathbf{X}_A - \mathbf{X}_{A'}$ possess the Gaussian distribution,

$$\langle \delta(\mathbf{r} - \mathbf{X}_A + \mathbf{X}_{A'}) \rangle = \frac{\exp(-r^2/(2D_{AA'}(t)))}{(2\pi D_{AA'}(t))^{3/2}}, \qquad D_{AA'}(t) \equiv \tfrac{1}{3} \left\langle (\mathbf{X}_A(t) - \mathbf{X}_{A'}(t))^2 \right\rangle , \tag{5}$$

where $D_{AA'}$ are the mean-squared distances between monomers. It is possible to exclude the effective potentials $V_{AA'}$ from the consideration and obtain closed differential equations for the correlations $\langle \mathbf{X}_A \mathbf{X}_{A'} \rangle_0$. At equilibrium these GSC equations become exactly the extrema conditions for the trial free energy, $\mathscr{A}_{trial} = \mathscr{A}_0 + \langle H - H_0 \rangle_0$ with $\mathscr{A}_0 = -k_B T \log \mathrm{Tr} \exp(-H/(k_B T))$ in the Gibbs–Bogoliubov variational principle.

The GSC equations are most conveniently written in terms of the mean-squared distances between monomers $D_{AA'}$, given by Eq. (5). Let us introduce the instantaneous free energy, $\mathscr{A}(t) = -T\mathscr{S} + \mathscr{E}$. For details of calculations we refer the reader to Refs. [5,11]. Here we present the final form of the kinetic GSC equations which describe the time evolution of the mean-squared distances between monomers (5),

$$\frac{1}{2}\frac{d}{dt} D_{AA'} = \sum_{B'} (\xi^{AB'} - \xi^{A'B'})(\Gamma_{AB'} - \Gamma_{A'B'}) , \tag{6}$$

$$\xi^{AA'} = \frac{\delta_{AA'}}{\zeta_b} + \frac{1 - \delta_{AA'}}{3(2\pi^3)^{1/2}\eta_s D_{AA'}^{1/2}}, \qquad V_{AA'} = -\frac{2}{3}\frac{\partial \mathscr{E}}{\partial D_{AA'}} , \tag{7}$$

$$\Gamma_{AA'} = -\frac{2}{3}\sum_{B'} D_{AB'} \frac{\partial \mathscr{A}}{\partial D_{A'B'}} = k_B T \delta_{AA'} + \sum_{B'} D_{AB'} V_{A'B'}, \tag{8}$$

where ζ_b and η_s are bare monomer friction and viscosity of the solvent, respectively. The entropy is given by the expression

$$\mathscr{S} = \tfrac{3}{2} k_B \log \det{}' R, \qquad R_{AA'} = \frac{1}{N^2}\sum_{BB'} D_{AB,A'B'} ,$$
$$D_{AA',BB'} \equiv -\tfrac{1}{2}(D_{AB} + D_{A'B'} - D_{AB'} - D_{A'B}) . \tag{9}$$

In Eq. (9) we have the determinant of the truncated matrix $R^{(N-1)}$ to exclude the zero eigenvalue related to the translational invariance for the centre of mass of the system. Let us introduce the total and partial radii of gyration,

$$\mathscr{R}^2 = \frac{1}{2N^2M^2}\sum_{AA'} D_{AA'}, \qquad \mathscr{R}_a^2 = \frac{1}{2N^2}\sum_{nn'} D_{nn'}^{aa} . \tag{10}$$

The mean energy may be written then as follows:

$$\mathscr{E} = \frac{3k_BT}{2L^2}M\left(\mathscr{R}^2 - \frac{1}{M}\sum_a \mathscr{R}_a^2\right) + \frac{3k_BT}{2l^2}\sum_{n,a} D^a_{n\,n-1} + \frac{3k_BT\lambda}{2l^3}\sum_{n,a}(D^a_{n+1\,n} + D^a_{n-1\,n} + 2D^a_{n+1\,n,n-1\,n}) + \sum_{J=2}^{\infty}\sum_{\{A\}}\hat{u}^{(J)}_{\{A\}}(\det\Delta^{(J-1)})^{-3/2}\,, \tag{11}$$

where $\Delta^{(J-1)}_{ij} \equiv D_{A_1A_{i+1},A_1A_{j+1}}$, and $\hat{u}^{(J)}_{\{A\}} \equiv (2\pi)^{-3(J-1)/2}u^{(J)}_{\{A\}}$. It is useful also to introduce the micro-phase separation (MPS) order parameter,[3] which describes the degree of correlation between matrices of the relative two-body interaction,[4] $(\sigma_A + \sigma_{A'})/2$, and the mean-squared distances, $D_{AA'}$.

3. Results

3.1. Kinetic laws at the collapse of the homopolymer

In Refs. [5,13] we have obtained the kinetic laws at the collapse of the ring homopolymer after one has instantaneously changed the quality of the solvent from the good ($u^{(2)} > 0$) to the bad ($u^{(2)} < 0$) regime. The GSC equations there have been transformed to $(N-1)/2$ independent Fourier modes, so their numerical solution can be achieved for systems of several hundreds of monomers.

For early times there is a spinodal stage with a characteristic power law decrease of the squared radius of gyration at very short times, $R_g^2(t) = R_g^2(0) - A_i\,t^{\alpha_i}$ with $\alpha_i = \frac{7}{11}$ $(\frac{9}{11})$. Here and below the first value of exponents is given without hydrodynamics ($\eta_s = \infty$), while the value in brackets corresponds to the regime of strong hydrodynamic interaction. The middle (coarsening stage) has the duration that scales as, $\tau_m \sim N^2\,|u_2'|^{-2}\,u_3(N^{3/2})$. The final relaxation (shape optimisation stage) is characterised by a slow exponential relaxation with the time scale,

$$R_g^2(t) = R_g^2(\infty) + A_f\,\exp\left(-\frac{t}{\tau_f}\right), \qquad \tau_f = \tau_1 = \frac{\zeta_1\mathscr{F}_1^{(e)}}{2k_BT} \sim N\mathscr{F}_1^{(e)}(N^{1/3}\mathscr{F}_1^{(e)})\,, \tag{12}$$

which gives the scaling, $\tau_f \sim N^{4/3}\,|u_2'|^{-2}\,u_3^{3/2}(N^{2/3})$.

In Ref. [5] we have suggested that for large N the GSC equations for an open homopolymer become equivalent to those of a ring with $N/2$ monomers and rescaled

[3] Defined as $\Psi = (N^2\,R_g^2\,2\Delta_\sigma)^{-1}\sum_{A,A'}(\sigma_A + \sigma_{A'})D_{AA'}$ where $(\Delta_\sigma)^2 = (1/NM)\sum_A \sigma_A^2$.

[4] In what follows we fix the units of temperature, size and time by choosing $k_BT = 1$, $l = 1$ and $\zeta_b = 1$. We account for the volume interactions up to the three-body terms, i.e. we assume that $u^{(J)}_{\{n\}} = 0$ for $J > 3$. Below we also fix the third virial coefficient, $u^{(3)} = 10$.

virial coefficients. However, as we mentioned there, this is merely an approximation since, strictly speaking, we cannot use the set of diagonal Fourier modes. We would like to briefly discuss here the differences in the folding kinetics between rings and open polymers exhibited in a more accurate treatment. Formally, we only need to remove the spring between the first and the last monomers in the effective free energy functional (2) to describe an open chain.

In Fig. 1 we present the typographic map of the $D_{mm'}$ matrix at various times during folding kinetics. Starting from some moment deeply inside the middle stage one clearly observes that the ends of the chain become quite different from the middle. Namely, in Fig. 1b, at long times after the quench, there are two distinct end clusters and the conformation here reminds that of a dumbell. This slowly compacts until it eventually produces a normal spherical globule in Fig. 1c. Such an effect is present for all values of the viscosity at sufficiently late times. However, the end clusters grow with about the same rate as the middle ones during the first and a considerable part of the middle kinetic stages. Interestingly enough, we find that the collapse time of an open chain is about 2–2.5 times longer than for the equivalent ring for chain lengths that we have studied.

Thus, although one may say that the ends play a special role in folding due to their higher freedom to move, the process of folding is not sped up by that, but is slowed down. This can be simply interpreted by observing an evolving polymer chain in Monte Carlo simulation [14]. Indeed, the chain is very tight during the middle stage when the end domination becomes significant. A ring chain pulls itself uniformly towards the centre thus helping the chain to collapse into a ball. On the contrary, an open chain has free end clusters which tend to be far from each other and it takes quite a long time for them to come into contact and coalesce eventually.

For considered system sizes we have also found that the kinetic exponents for an open homopolymer obtained by fitting remain in good agreement with the scaling laws discussed above for rings. This implies that the end effects do not change the dominant collapse mechanism – midchain clusters grow mostly at the expense of absorbing the slack and neighbouring clusters along the chain.

3.2. Equilibrium structures of a single copolymer

In studying equilibrium one considers the stationary points of Eq. (6) and the variational free energy. The deepest minimum of the free energy corresponds to the thermodynamically stable state, the rest of the solutions to metastable states. For simplicity here we consider copolymers with the ring topology.

Typical phase diagrams are presented in Figs. 2 and 3. In the region $\bar{u}^{(2)} > 0$ and for small values of amphiphilicity the conformation is akin to the homopolymer extended coil. By decreasing $\bar{u}^{(2)}$ to the negative region the chain undergoes the continuous collapse transition, which similarly to the homopolymer, is characterised by a rapid fall of the radius of gyration, R_g^2, and the change of the fractal dimension.

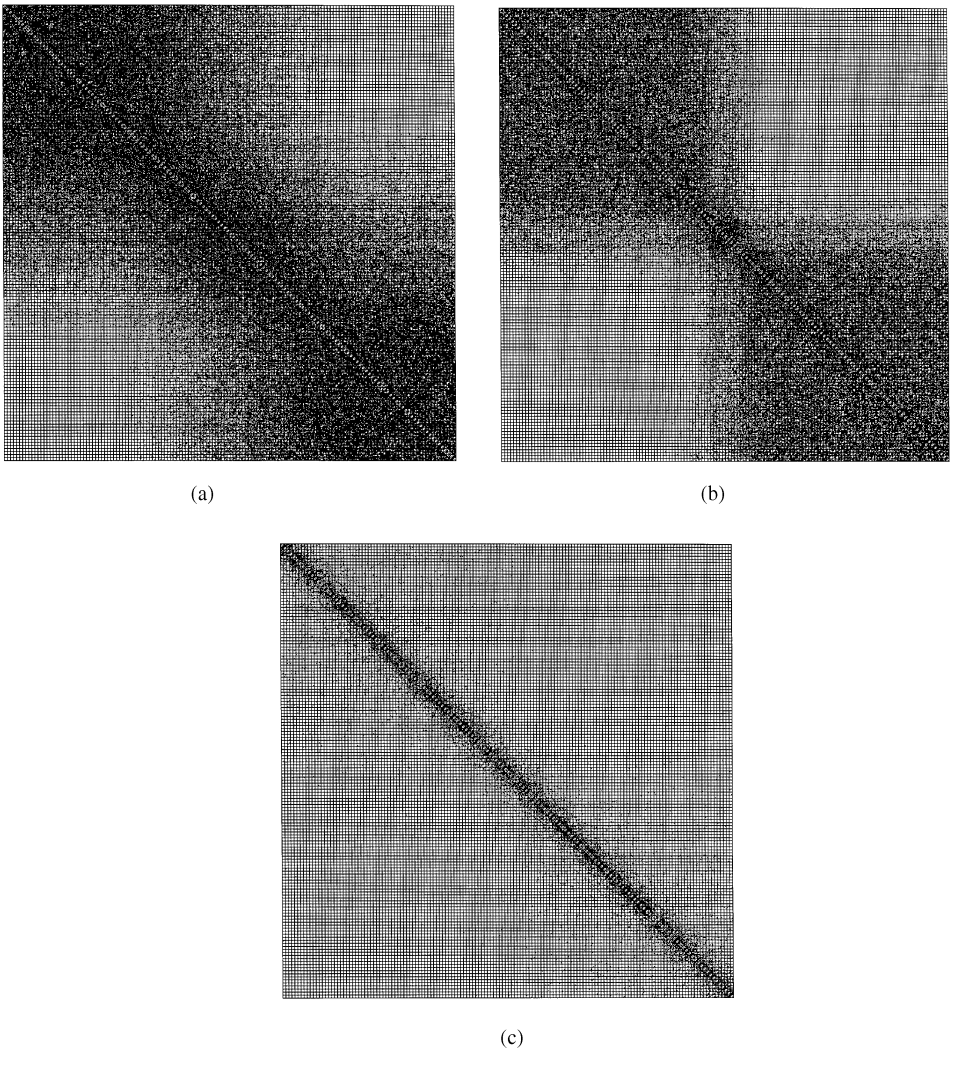

Fig. 1. Diagrams of the mean-squared distances matrix, $D_{mm'}$ for open homopolymer with $N = 150$, in kinetics after the quench, $u^{(2)} = 30 \to -50$. Here $\eta_s = 0.1$. Diagrams (a)–(c) correspond, respectively, to the following moments in time: $t = 27$, 52 and 73.0. Indices m, m' start counting from the upper left corner. Each matrix element, $D_{mm'}$ is denoted by a quadratic cell with varying degree of black colour, the darkest and the lightest cells corresponding, respectively, to the smallest and to the largest mean-squared distances. The diagonal elements are not painted since by definition, $D_{mm} = 0$.

The collapse transition for larger values of amphiphilicity turns out to be more complicated, and essentially depends on the sequence. The globular state for large values of Δ is different from the liquid-like globule. It is characterised by somewhat higher value of R_g^2 and a very large value of the MPS order parameter, so we call it the MPS globule. This state is separated from the liquid-like globule by a weak

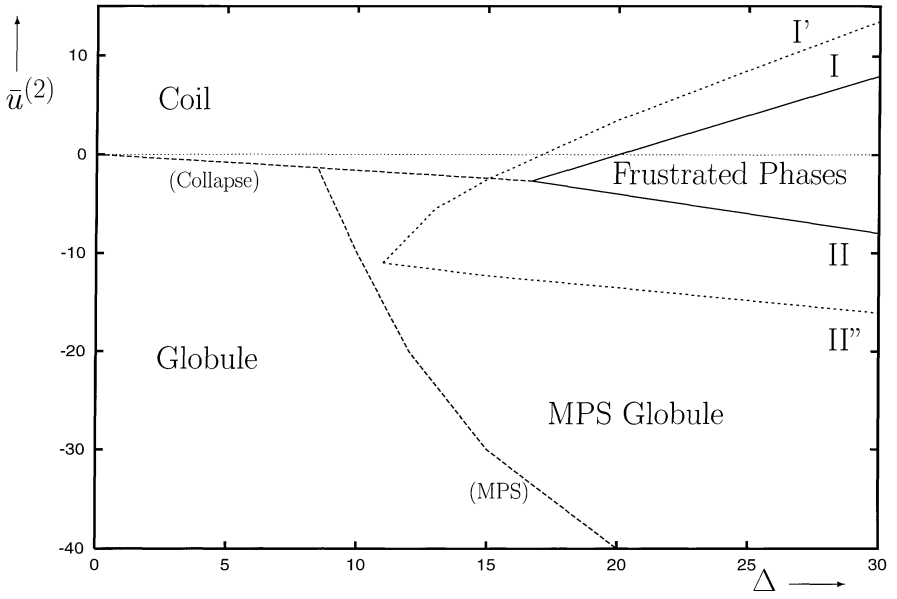

Fig. 2. The phase diagram of the sequence "$babca_2cbac_2acb_3cac_3a_2b_2cac_2b$" in terms of the mean second virial coefficient, $\bar{u}^{(2)}$, and the amphiphilicity, Δ. Curves (Collapse) and (MPS) correspond respectively to the collapse and the micro-phase separation continuous transitions. Curves (I) and (II) correspond to discontinuous transitions to the frustrated phases. "Spinodal" curves (I') and (II") bound the regions of metastability of the frustrated states. Transition curves and boundaries distinguishing different frustrated states are not depicted.

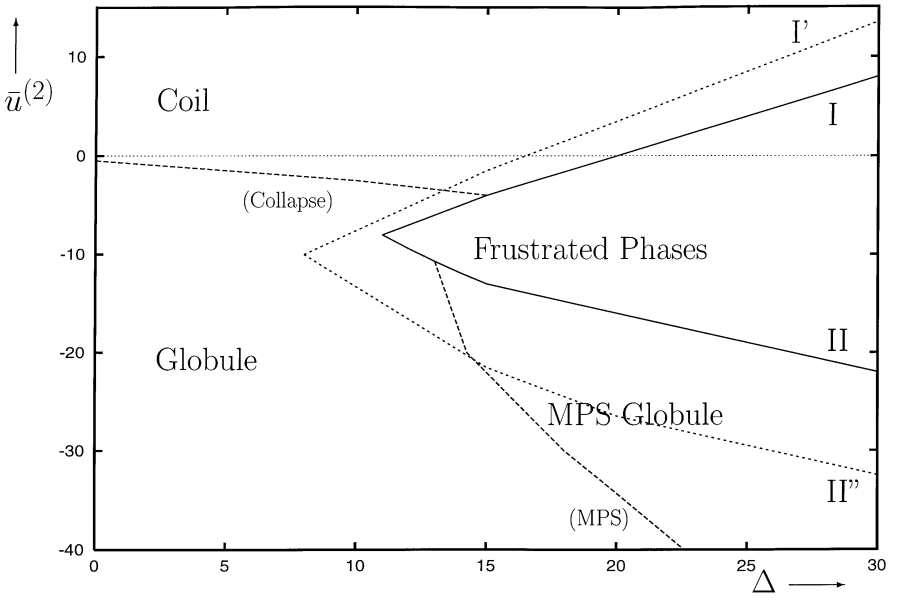

Fig. 3. The phase diagram of the sequence "$(babca_2cbac_2acb_3cac_3a_2b_2cac_2b)_2$", i.e. twice as in Fig. 2 in terms of the mean second virial coefficient, $\bar{u}^{(2)}$, and the amphiphilicity, Δ.

continuous transition. Note that for long blocks (see Ref. [13]) the collapse transition to the MPS globule becomes discontinuous.

However, for a wide class of sequences starting from some value of Δ in an intermediate region of $\bar{u}^{(2)}$ there appear additional solutions corresponding to local minima of the free energy. The broad region where this could take place is bounded by the curves I' and II" in Figs. 2 and 3. With increasing Δ the number of such solutions grows very quickly. Significantly, in the region of the phase diagram, between curves I and II in Figs. 2 and 3, some of these possess the lowest free energy value, this being the thermodynamically stable state. Since the number of such solutions is rather large even for short sequences, we shall call them collectively the *frustrated phases*.

Now let us compare the phase diagrams in Figs. 2 and 3, the latter corresponding to the sequence twice longer than for the former. An interesting observation is that the region between spinodals I' and II", designating where the frustrated phases can exist, expands dramatically with increasing chain length. The same is true for the region of thermodynamically stable frustrated phases between curves I and II. For rather long chains we may expect that the regions of stability and metastability of the frustrated phases will continue to expand downwards and to the left, so that the lines II and II" will become nearly vertical, displacing the region of stable MPS globule. The diversity and a special foliating structure of various branches lead in the thermodynamic limit to what is known as a spin glass frozen phase [15] of random copolymers.

3.3. Folding kinetics of a single copolymer

Here we shall consider the time evolution of a copolymer away from the initial equilibrium after a quench from the homopolymer coil, where all monomers are equally hydrophilic ($\bar{u}^{(2)} = 15$ and $\Delta = 0$), to the region of the MPS globule, so that the "a" species became strongly hydrophobic and the "b" species remained nearly neutral ($\bar{u}^{(2)} - 35$ and $\Delta = 30$).

The time evolution of the radius of gyration, $R_g^2(t)$, and the instantaneous free energy, $\mathscr{A}(t)$, is presented in Fig. 4. Here line A corresponds to the homopolymer, for which R_g^2 and $\mathscr{A}$ decrease monotonically to the equilibrium values corresponding to the liquid-like globule. As for the copolymer kinetics, the first observation is that it proceeds much slowly than for the homopolymer. For example, for the simplest copolymer sequence, "$(ba)_{25}$", the total collapse time (see Section 3.1) is more than 3 times longer than that of the homopolymer, other copolymer sequences collapsing even longer.

The evolution of the instantaneous free energy (Fig. 4b) proceeds through multiple accelerations and decelerations. The flat regions of a staircase-like function correspond to temporary kinetic arrest of the system in transient nonequilibrium conformations, i.e. to transient trappings of various members of the ensemble in their local shallow energy minima. Since such minima are encountered at different moments in time for different members of the ensemble, their influence on the overall time evolution of averaged observables is manifested in a smooth characteristic slowing down. Note here that the number of steps in kinetics process hardly can be guessed from the given

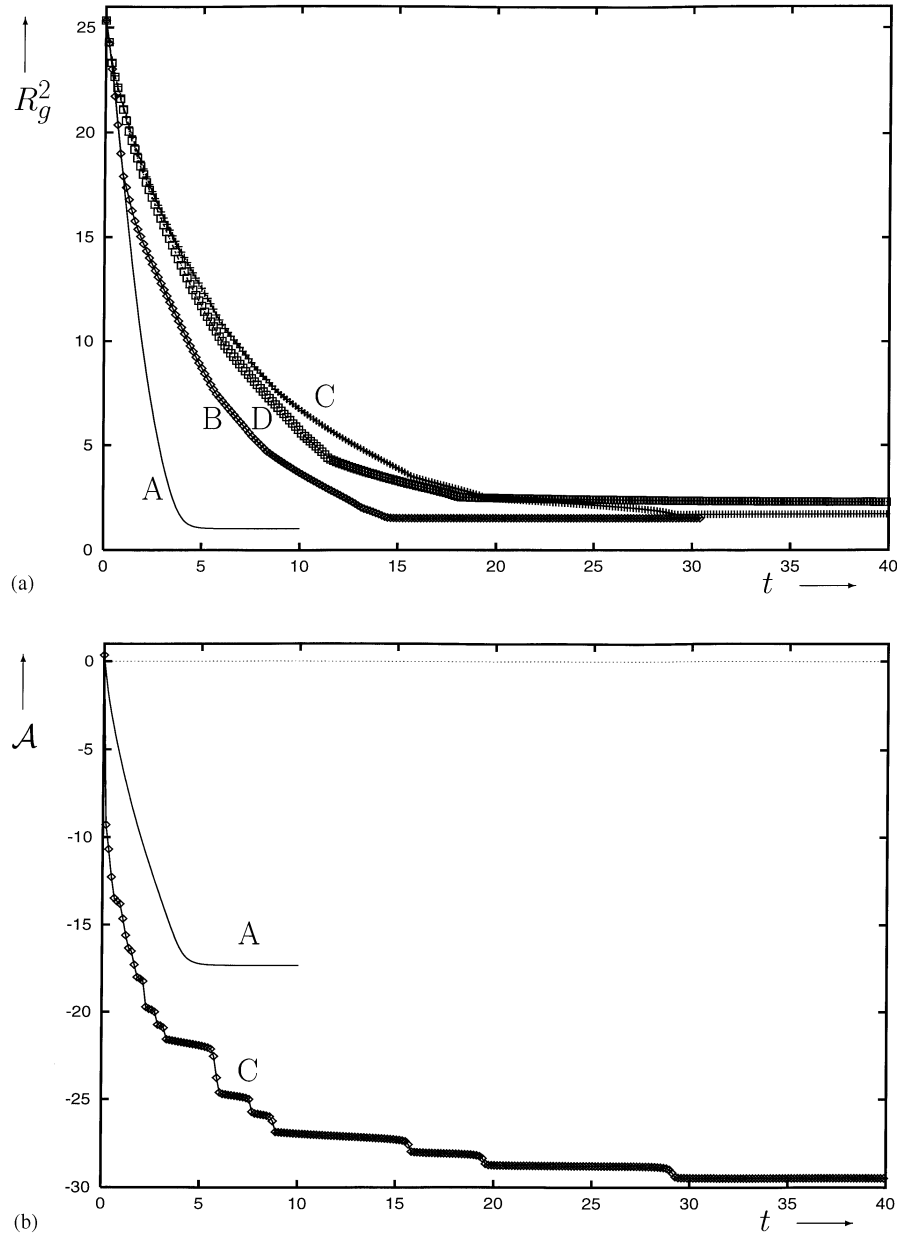

Fig. 4. Plot of the mean-squared radius of gyration, R_g^2 (a) and the instantaneous free energy, $\mathscr{A}$ (b) vs. time, t, during kinetics after the quench from $\bar{u}^{(2)} = 15$, $\Delta = 0$ to $\bar{u}^{(2)} = -35$, $\Delta = 30$ for copolymer sequences with $N = 50$. Lines A–D in the figures correspond, respectively, to the following sequences: "c_{50}" (homopolymer), "$(ba)_{25}$", "$a_2b_3a_3b_2a_3b_2a_2b_3(ba)_{15}$" and "$(ba)_3b_2(ba)_9a_2(ba)_5b_2a_2(ba)_4$".

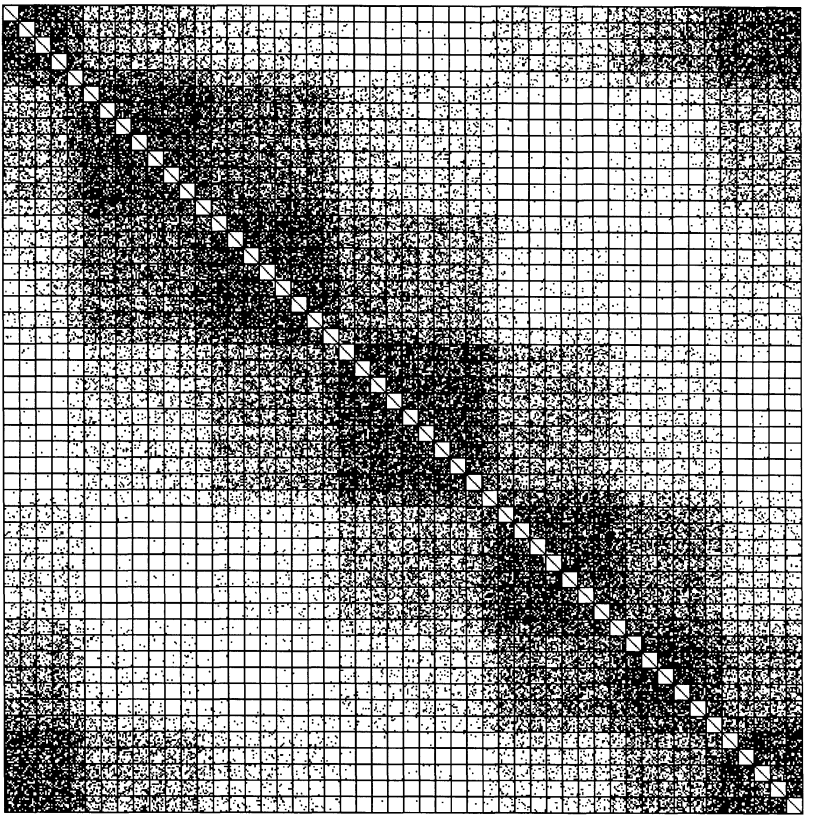

Fig. 5. Diagram of the mean-squared distances matrix, $D_{mm'}(t)$ for "$(ba)_{25}$" copolymer in kinetics after the same quench as in Fig. 4 at time moment $t = 5.75$.

primary sequence. Typically, the kinetics for sequences with smaller number of blocks proceeds through smaller number of steps.

Now, let us consider the nonequilibrium conformation given by the matrix of the mean squared distances between monomers, $D_{mm'}$. We can see that kinetic process proceeds through formation of locally collapsed and phase-separated clusters (see Fig. 5). During later evolution these clusters approach each other until eventually they unify forming the MPS globule. For the latter the $D_{AA'}$ matrix has a chess-board-like appearance, so that its structure strongly resembles that of the $u^{(2)}_{AA'}$ matrix away from the diagonal (see Ref. [13]). Note also that these nonequilibrium states do not possess the translational block symmetry, present for the system in the Hamiltonian and the initial conditions. After some time in kinetics, $t \approx 1$ this symmetry breaks down, and restores only during final kinetic stages $t \approx 15$.

Finally, let us discuss how the folding kinetics depends on the sequence. In Fig. 4 we present kinetic processes for the simplest copolymer consisting of "*ab*" blocks (sequence B), and also for some sequences obtained by certain modifications in it.

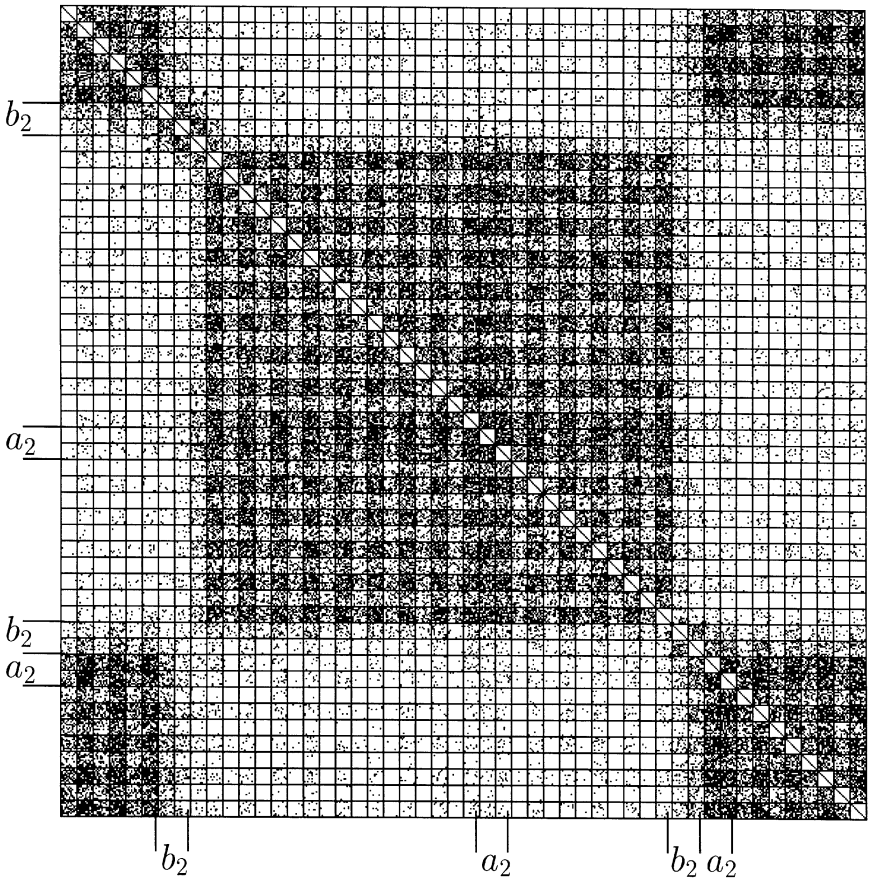

Fig. 6. The diagram of the mean-squared distances matrix, $D_{mm'}(t)$ for copolymer sequence "$(ba)_3b_2(ba)_9a_2(ba)_5b_2a_2(ba)_4$" at the time moment $t=45$, so that this conformation is close to the final equilibrium. Parameters of the quench are the same as in Fig. 4.

In the sequence denoted by C we have replaced ten short blocks by four of longer size. In the sequence D we have inserted only two hydrophobic and two hydrophilic fragments into the sequence, i.e. we have made only two permutations. For the former sequence the total kinetic time becomes approximately 1.7 times longer than that for the B sequence. The final values of the free energy for both sequences B and C are nearly the same, whilst the micro-phase separation is higher for the modified sequence C due to longer blocks. Thus, for that sequence the kinetic properties do not deteriorate very much, except that the kinetic process takes much longer. However, the kinetic foldability of the D sequence is much poorer than for B and C sequences. In fact, here not only the kinetic process takes much longer, but the final state is different from the MPS globule. As one can see from Fig. 6 the final kinetic state for the D sequence consists of two clusters. These clusters are connected by two links, formed by nearly

neutral fragments, "b_2". Further collapse of this conformation is unfavorable due to the entropy and partial screening of hydrophobic monomers by nearly neutral species "b". Size of such *misfolded* state is larger and the MPS order parameter is approximately twice smaller than one would expect for the MPS globule.

3.4. Formation of mesoglobules at low concentration

In Ref. [8] we have studied the GSC equations for solution of identical ring homopolymers upon an additional assumption that the mean-squared distances between any two monomers from different chains are all equal to each other. In addition to the equations for a single chain, we have an equation describing the evolution of inter-chain distance. Number of chains, M, here appears as a parameter in equations.

The phase diagram obtained in this way (Fig. 1 in Ref. [8]) has the two-phase coexistence region in agreement with the standard Flory–Huggins theory. The curve of vanishing $\partial^2\mathscr{A}/\partial M^2$ there (curve II) corresponds to the spinodal of two-phase separation. Naturally, there are two pure states for negative $u^{(2)}$: the gas of single globules and the precipitate. The transition between the two is of the first-order up to the semidilute regime (curve I) terminating in a critical point (A) of a liquid–gas type, then at higher concentrations the transition from the swollen coils to the precipitate becomes continuous (curve II). Note that, since we have a first-order transition, there are two "spinodals" (I' and I") corresponding to the transition curve (I), which designate the boundaries of existence of the metastable precipitate and the metastable gas of single globules, respectively. An important observation is that the free energy is concave with respect to M at both branches in the two-phase coexistence region. Thus, we have used the Maxwell construction for both the stable and the metastable branches. While the former produces the conventional two-phase coexistence picture of the high- and low-density phases, the latter has led us to believe that in the region between the transition curve (I) and the lower "spinodal" (I") there appears a metastable coexistence of interacting gas of *mesoglobules*, obtained by collapse of a few distinct chains, with a gas of single chain globules.

Now, we can prove this directly. The extended GSC method can describe formation of mesoglobules since it is possible to distinguish the mean-squared distances between various chains. In Fig. 7 we present the mean-squared radius of clusters corresponding to various stationary points of Eq. (6) for four chains in a box. The curves 1×4 and 4×1 correspond to the precipitate (macroglobule from four chains) and four single-chain globules, respectively, with I being the point of phase transition between them. Detailed analysis shows that there are also other stationary points (local minima of the free energy), such as curve $1+3$ (1 single chain globule and 1 globule from three chains) and curve $2+2$ (two mesoglobules from 2 chains), which are displayed as long as they exist. For a given $u^{(2)}$ these branches have a somewhat higher value of the free energy, and hence they are metastable states. The difference in the free energy values between these and thermodynamically dominant states, however, is rather small, but the barriers between them are quite high. Therefore, if the system is trapped in one

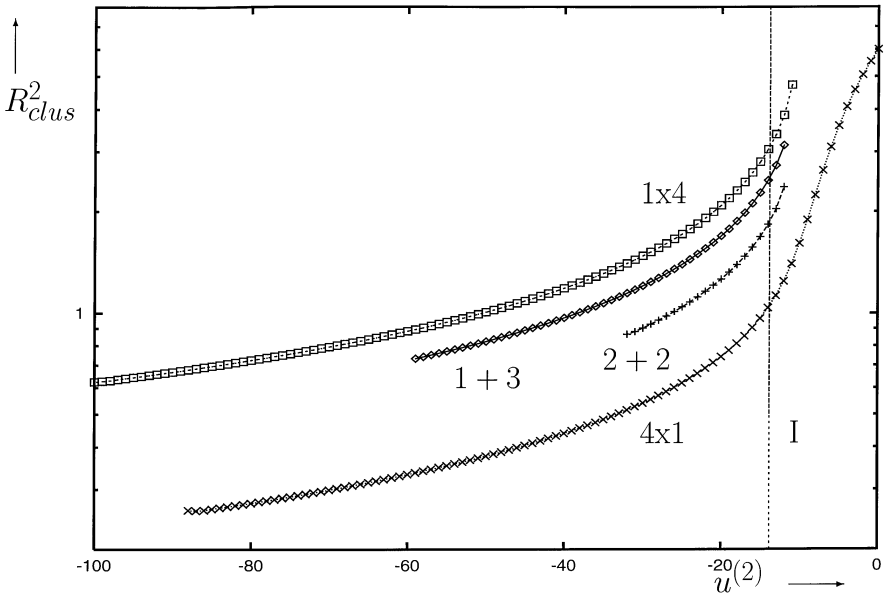

Fig. 7. Plot of the mean-squared cluster size for different states. This data is obtained for open homopolymers with $N = 18,\ M = 4,\ L = 10$.

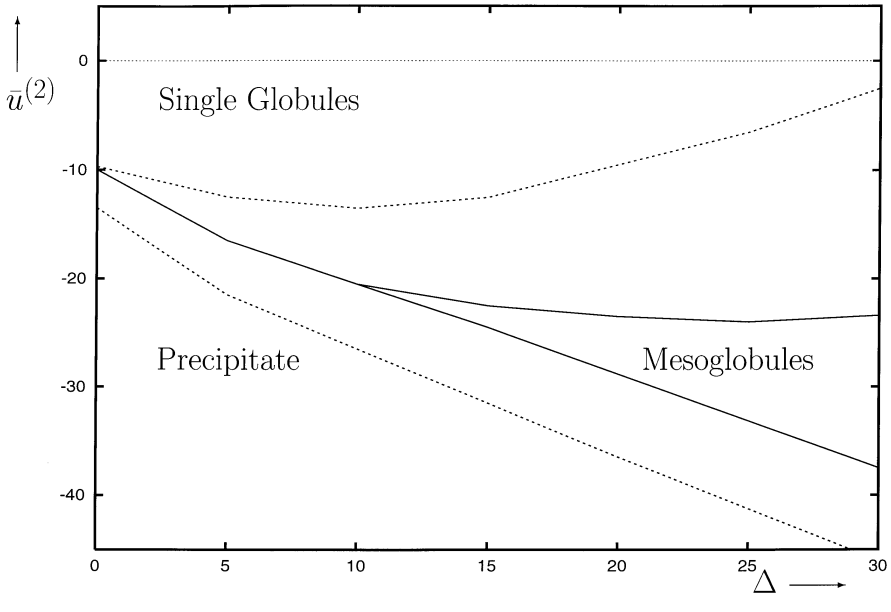

Fig. 8. Phase diagram for solutions of $(ab)_9$ copolymers in variables of the amphiphilicity, Δ, and the mean second virial coefficient, $\bar{u}^{(2)}$, for polymers with $N = 18,\ M = 4,\ L = 5$. Only thermodynamically stable states are displayed.

of such states, it remains there for a long time. Another important conclusion is that among different types of a few chain clusters those having equal size possess the lowest free energy. Thus, the metastable mesoglobules have a thermodynamic preference to be of equal size. In practice, this would lead to a rather monodisperse distribution of mesoglobule sizes, but only in a rather narrow region at low concentrations around the transition I.

In Fig. 8 we present the phase diagrams at a fixed concentration for the solution of periodic $(ab)_9$ copolymers. For small amphiphilicity parameter Δ we find a picture quite similar to the homopolymer. However, for higher values of Δ the $2+2$ minimum of mesoglobules becomes the main free energy minimum in a narrow region designated as 'Mesoglobules' in Fig. 8, with the surrounding transitions to other phases being naturally first order. Such a phase diagram turns out to be quite typical for other more complicated copolymer sequences. Thus, the mesoglobules that exist in the first place due to a delicate balance of the volume interactions and the entropy resisting further aggregation, are further stabilised by the micro-phase separation in copolymers. Their size is related to the mesoscale at which the micro-phase separation is more preferable.

4. Discussions and conclusion

In this work we have presented the extended Gaussian self–consistent method for any number of chains of any composition and with arbitrary topology. In particular, the following problems are considered:

We discuss the influence of the chain topology on the folding process. The comparison of the open chain vs. the ring has been a matter of some controversy in the literature [16,17] and we hope to have shed some new light on this here. Namely, we find that the folding of an open chain is slower than that of an equivalent ring. The end clusters are found to be the largest during most of the coarsening stage. Despite this special role of the ends, the attending kinetic laws of folding are characterised by the same exponents as for a ring chain.

We carry out a detailed analysis of various conformational structures that could be formed in solution of amphiphilic copolymers and study the transitions between them. A typical phase diagram of a random copolymer contains from phases of the coil, the liquid-like globule, the micro-phase separated globule and a large number of frustrated partially misfolded states. The latter are related to the frozen phase of the spin-glass-type systems. Most of these states are metastable and can be classified by the number and sizes of micro-phase separated clusters of monomers that constitute the conformation.

A similar analysis is carried out for solutions at higher concentrations. Special attention is payed to the thermodynamic stability of the monodisperse mesoglobules observed in recent experiments. We believe that the entropic barriers dependent on the conformational state of the chain, i.e. the amount of water surrounding monomers, may explain the additional stabilisation of mesoglobules in PNIPAM solution [10,12].

The work on dilute copolymer solutions is ongoing in a number of laboratories around the world. One may expect many interesting new findings in this area with improving experimental techniques. We hope that variational approaches, and the GSC method of the nonequilibrium statistical mechanics in particular, although more computationally expensive than mean-field theories, can assist a great deal in fundamental understanding of results from such experiments.

Acknowledgements

We are grateful to Professor K. Kawasaki, Professor G. Parisi, and our colleagues Dr A.V. Gorelov and A. Moskalenko for interesting discussions. We also acknowledge the support of the Centre for High Performance Computing Applications, University College Dublin, Ireland.

References

[1] P.G. de Gennes, Scaling Concepts in Polymer Physics, Cornell University Press, New York, 1988; J. des Cloizeaux, G. Jannink, Polymers in Solution, Clarendon Press, Oxford, 1990; M. Doi, S.F. Edwards, The Theory of Polymer Dynamics, Oxford Science, New York, 1989; A.Yu. Grosberg, A.R. Khokhlov, Statistical Physics of Macromolecules AIP, New York, 1994.
[2] D.R. Paul, S. Neuman (Ed.), Polymer Blends, Academic Press, 1987; I.S. Miles, S. Rostami (Eds.), Multicomponent Polymer Systems, Longman Scientific and Technical, Singapore, 1992.
[3] M. Daoud, G. Janninck, J. Phys. (Paris) 37 (1976) 973; F. Tanaka, J. Chem. Phys. 82 (1995) 4707; B. Duplantier, J. Phys. (Paris) 43 (1982) 991; Europhys. Lett. 1 (1986) 491; A.Yu. Grosberg, D.V. Kuznetsov, Macromolecules 25 (1992) 1991.
[4] G. Allegra, F. Ganazzoli, J. Chem. Phys. 83 (1985) 397; G. Raos, G. Allegra, J. Chem. Phys. 104 (1997) 1626.
[5] E.G. Timoshenko, Yu. A. Kuznetsov, K.A. Dawson, J. Chem. Phys. 102 (4) (1995) 1816; E.G. Timoshenko, Yu. A. Kuznetsov, K.A. Dawson, J. Chem. Phys. 104 (9) (1996) 3338; Phys. Rev. E 53 (4) (1996) 3886; E.G. Timoshenko, Yu. A. Kuznetsov, K.A. Dawson, J. Chem. Phys. 54 (4) (1996) 4071.
[6] P.J. Flory, J. Chem. Phys. 9 (1941) 660; M.L. Huggins, J. Chem. Phys. 9 (1941) 440; D.J. Meier, J. Polym. Sci. C26 (1969) 81; T. Ohta, K. Kawasaki, Macromolecules 19 (1986) 2621; L. Leibler, Macromolecules 13 (1980) 1602.
[7] J. Yu, Z. Wang, B. Chu, Macromolecules 25 (1992) 1618; B. Chu, Q. Ying, A.Yu. Grosberg, Macromolecules 28 (1995) 180.
[8] E.G. Timoshenko, Yu. A. Kuznetsov, K.A. Dawson, Phys. A 240 (1997) 432.
[9] Y. Deng, R. Pelton, Macromolecules 28 (1995) 4617.
[10] A.V. Gorelov et al., Il Nuovo Cimento. D 16 (1994) 711; A.V. Gorelov, A. du Chesne, K.A. Dawson, Phys. A 240 (1997) 443.
[11] E.G. Timoshenko, Yu.A. Kuznetsov, K.A. Dawson, in: F. Mallamace (Ed.), Proc. of the Int. Conf. on Morphology and Kinetics of Phase Separating Complex Fluids, Messina, Italy, 1997; Phys. Rev. E 1998, in press.
[12] X. Qiu, C.M.S. Kwan, C. Wu, Macromolecules 30 (1997) 6090.
[13] Yu.A. Kuznetsov, E.G. Timoshenko, K.A. Dawson, in: F. Mallamace (Ed.), Proc. Int. Conf. on Morphology and Kinetics of Phase Separating Complex Fluids, Messina, Italy, 1997.
[14] Yu.A. Kuznetsov, E.G. Timoshenko, K.A. Dawson, J. Chem. Phys. 103 (1995) 4807.
[15] M. Mezard, G. Parisi, M. Virasoro, Spin Glass Theory and Beyond, World Scientific, Singapore, 1987.
[16] B. Ostrovsky, Y. Bar-Yam, Comp. Pol. Sci. 3 (1993) 9.
[17] A. Buguin, F. Brochard-Wyart, P.G. de Gennes, C.R. Acad. Sci. Paris 322 (S.IIb) (1996) 741.